Enhancement of thermoelectric efficiency in a two-level molecule

2010 J. Phys.: Condens. Matter 22 185302

(http://iopscience.iop.org/0953-8984/22/18/185302)

J. Phys.: Condens. Matter **22** (2010) 185302 (8pp) doi:10.1088/0953-8984/22/18/185302

Enhancement of thermoelectric efficiency in a two-level molecule

M Wierzbicki and R Świrkowicz

Faculty of Physics, Warsaw University of Technology, ulica Koszykowa 75, 00-662 Warsaw, Poland

Received 25 January 2010, in final form 25 March 2010
Published 20 April 2010
Online at stacks.iop.org/JPhysCM/22/185302

Abstract
Electron and energy transport through a two-level molecule (quantum dot) with intra- and inter-level Coulomb correlations is studied using the non-equilibrium Green function formalism. Thermoelectric coefficients are determined in the regime of linear transport for a wide range of gate voltages and temperature. At low temperatures Coulomb blockade effects lead to oscillations of thermal conductance which are well correlated with oscillations in electron conductance. Due to different probabilities of particular one- and two-particle configurations, the intensities of the peaks corresponding to resonant states are different, which results in the selection of channels active in the transport. Additional selection can be obtained for molecules with level-dependent tunnelling rates to external electrodes. In such systems, channels with strongly reduced heat transfer can appear, which results in an enhancement of the thermal efficiency.

1. Introduction

Thermoelectric effects in low dimensional structures and nanoscale systems have been recently widely investigated in view of future applications of energy conversion devices in nanoelectronics [1–11]. Studies of nanosystems also offer a new insight into the Coulomb blockade effect and are related to novel phenomena which are of fundamental interest. Enhanced thermoelectric efficiency was reported for new materials [1–5], silicon nanowires [7, 9] as well as for molecular junctions [12, 13]. The tendency of a system towards thermoelectricity is described by the thermoelectric figure of merit $ZT = S^2GT/\kappa$, where T denotes the temperature, G and κ represent the electrical and thermal conductance, and S is the Seebeck coefficient, which is defined as the ratio of the voltage drop ΔV generated by the temperature difference ΔT. The high values of ZT measured in new materials can be attributed to suppression of the lattice thermal conductance [1–5]. Small contributions to κ due to phonons are also expected in nanostructures containing quantum dots (QD) and molecular junctions [6, 12]. In single-electron devices a violation of the Wiedemann–Franz law is observed and it can account for the enhancement of the thermoelectric efficiency [12, 13]. Giant magnetothermoelectric power was measured in multilayered nanopillars [14]. The Seebeck coefficient was investigated in a variety of nanoscale systems such as atomic-size wires [15], Si nanowires [7, 9], quantum dots [16] and molecular junctions [6, 8].

Many theoretical approaches have been proposed to study thermoelectric effects in nanostructures [12, 13, 17–39]. The figure of merit was investigated for molecular junctions within density functional theory, and a strong enhancement of thermoelectric efficiency was found [13]. Model calculations were used to study electron and energy transport through Coulomb islands [24–30, 37] and single-level quantum dots in the Coulomb blockade [17, 38, 39] as well as in Kondo regimes [31–36]. Oscillations of electron thermal conductance κ, similar to those in electrical conductance, were obtained for Coulomb islands [24, 29, 30, 37]. The effects of the interplay between the charging energy, thermal energy and the confinement on Coulomb oscillations were discussed [30, 37]. In the quantum limit the periodicity of the oscillations of thermal conductance is the same as in the Coulomb blockade oscillations of the conductance G, but the intensities of peaks in κ are smaller than those predicted by the Wiedemann–Franz law [30]. The dependence of κ on the energy level spacing ΔE and the thermal energy shows that quantum confinement is responsible for the fast decrease of electron thermal conductance of the dot. The thermopower of a QD also oscillates as a function of a gate voltage [24, 27]. The shape of the peaks strongly depends on temperature. In the quantum regime with ΔE higher than kT, an additional fine structure can develop [27].

The interplay between thermoelectric and spin effects in the Coulomb blockade regime was studied for a single-level QD coupled to ferromagnetic electrodes [38, 39]. It was found that thermopower as well as figure of merit depend on the magnetic configuration of the system [39].

In the present paper we use the non-equilibrium Green function formalism to study the thermoelectric properties of a multilevel quantum dot/molecule as well as two coupled dots. Applying the method proposed by Chang and Kuo [40, 41] we take into account the probabilities of single and two particle configurations in a multilevel dot with intra- and inter-level Coulomb correlations. The probabilities strongly influence the peak intensities in electrical and thermal conductance leading to the selection of channels active in the transport. Additional selection of channels can be obtained for a molecule with two orbital levels coupled to the leads with considerably different coupling strengths. The possibility of selection of accessible channels allows us to achieve regimes in which the thermal conductance is considerably suppressed, whereas the thermopower can be enhanced. In such conditions high thermoelectric efficiency can be obtained. Changes of the thermoelectric properties of two quantum dots, when the inter-dot coupling strength is tuned, are also discussed.

2. Electron and energy transport in Green function formalism

The system to be considered consists of a quantum dot or a molecule attached to external electrodes and is described by the Hamiltonian: $H = H_{\mathrm{D}} + H_{\mathrm{e}} + H_{\mathrm{T}}$. The first term H_{D} takes the form

$$H_{\mathrm{D}} = \sum_{i\sigma} \varepsilon_i d^{\dagger}_{i\sigma} d_{i\sigma} + \tfrac{1}{2} \sum_{ij\sigma\sigma'} U_{ij} d^{\dagger}_{i\sigma} d_{i\sigma} d^{\dagger}_{j\sigma'} d_{j\sigma'} \qquad (1)$$

and corresponds to the central region in a form of small QD with discrete levels $\varepsilon_i = \varepsilon_{i0} + eV_{\mathrm{g}}$ active in transport. Level positions can be tuned using the gate voltage V_{g}. On site intra-level as well as inter-level Coulomb interactions are described by the second term in H_{D} (equation (1)) and U_{ij} represent the appropriate Hubbard parameters. $d^{\dagger}_{i\sigma}$ ($d_{i\sigma}$) denotes here the creation (annihilation) operator of an electron on the dot in the state $i\sigma$.

The term $H_{\mathrm{e}} = \sum_{\beta=\mathrm{L,R},k\sigma} \varepsilon_{k\beta} c^{\dagger}_{k\beta\sigma} c_{k\beta\sigma}$ corresponds to the left ($\beta = \mathrm{L}$) and right ($\beta = \mathrm{R}$) electrodes, in which electrons are treated as non-interacting particles with energy $\varepsilon_{k\beta}$. The two leads are assumed to be in local equilibrium with temperature T_β and chemical potential μ_β. Tunnelling processes between the central part and the electrodes are described by the third term in the Hamiltonian H, which is taken in a standard form: $H_{\mathrm{T}} = \sum_{\beta ki\sigma} (V^{\beta}_{ki} c^{\dagger}_{k\beta\sigma} d_{i\sigma} + V^{*\beta}_{ki} d^{\dagger}_{i\sigma} c_{k\beta\sigma})$. V^{β}_{ki} are elements of the tunnelling matrix corresponding to the level i.

Electric and heat currents induced due to presence of a small voltage $\Delta V = \frac{1}{e}(\mu_{\mathrm{L}} - \mu_{\mathrm{R}})$ and temperature gradient $\Delta T = T_{\mathrm{L}} - T_{\mathrm{R}}$ can be written as (see e.g. [42]): $I = e^2 L_0 \Delta V + \frac{e}{T} L_1 \Delta T$, $I_Q = -eL_1 \Delta V - \frac{1}{T} L_2 \Delta T$ with $L_n = -\frac{1}{h} \int \mathrm{d}E T(E)(E-\mu)^n \frac{\partial f}{\partial E}$. f denotes here the Fermi–Dirac distribution function. Transmission $T(E)$ is given in the form: $T(E) = \sum_{j\sigma} \Gamma^{\mathrm{L}}_j \Gamma^{\mathrm{R}}_j / (\Gamma^{\mathrm{L}}_j + \Gamma^{\mathrm{R}}_j) i(G^{\mathrm{r}}_{j\sigma} - G^{\mathrm{a}}_{j\sigma})$ and $G^{\mathrm{r(a)}}_{j\sigma}$ represents the Fourier transform of the appropriate Green function. Γ^{β}_j defined as $\Gamma^{\beta}_j = 2\pi \sum_k |V^{\beta}_{kj}|^2 \delta(E - \varepsilon_{k\beta})$ describes coupling of the dot level j with the electrode β. In the following it is assumed in the form: $\Gamma^{\beta}_j = \Gamma[1 - (-1)^j Q]$ with Γ treated as a parameter independent of energy. Moreover, we limit the discussion to the two-level system with $j = 1, 2$, while $0 \leqslant Q < 1$ describes the coupling strength of a given level with electrodes. For $Q = 0$ both levels are coupled with electrodes with the same strength Γ. As Q increases, the level with $j = 1$ becomes strongly coupled to both electrodes, whereas the second one with $j = 2$ is weakly coupled; their couplings are described by $\Gamma^{\beta}_1 = \Gamma(1+Q)$, $\Gamma^{\beta}_2 = \Gamma(1-Q)$, respectively.

To determine Green functions $G_{j\sigma}(E) = \langle\langle d_{j\sigma}, d^{\dagger}_{j\sigma}\rangle\rangle$ the equation of motion method is used. This approach, which allows one to find expressions for $G_{j\sigma}$ in QD-systems with multiple energy levels in the Coulomb blockade regime, was recently proposed by Chang and Kuo [40] and will be applied here to study electron and heat transfer. Following this procedure we write the retarded Green function in the form:

$$G^{\mathrm{r}}_{j\sigma}(E) = \sum_{k=0}^{2} p_k \left(\frac{1 - n_{j-\sigma}}{E - \varepsilon_j - A_k - \Sigma^{\mathrm{r}}_j} + \frac{n_{j-\sigma}}{E - \varepsilon_j - U_j - A_k - \Sigma^{\mathrm{r}}_j} \right). \qquad (2)$$

The summation is over possible configurations with the level $l = -j$ ($l = 2$ for $j = 1$ and $l = 1$ for $j = 2$) occupied by zero, one or two particles, respectively. p_k denotes here the probability factor of a given configuration k and is determined by the average one-particle occupation numbers $n_{l\sigma} = \langle d^{\dagger}_{l\sigma} d_{l\sigma}\rangle$ and two-particle occupations $c_{l\sigma} = \langle n_{l-\sigma} n_{l\sigma}\rangle$ in a following way: $p_0 = 1 - (n_{l\sigma} + n_{l-\sigma}) + c_{l\sigma}$, $p_1 = n_{l\sigma} + n_{l-\sigma} - 2c_{l\sigma}$, $p_2 = c_{l\sigma}$. They give, respectively, the probability of the configuration with no particle, with one and two particles in the level l different from j. On the other hand, the level j, through which the electron can tunnel, can be empty (with probability $1 - n_{j-\sigma}$) or singly occupied with probability $n_{j-\sigma}$. A_k in the denominator denotes the sum of all interactions seen by the electron in the level j due to other particles occupying the level $l = -j$ in configuration k, $A_0 = 0$, $A_1 = U_{jl}$ and $A_2 = 2U_{jl}$. The occupation numbers $n_{l\sigma}$ and $c_{l\sigma}$ are expressed in terms of lesser Green functions: $n_{l\sigma} = -\mathrm{i} \int \frac{\mathrm{d}E}{2\pi} \langle\langle d_{l\sigma}, d^{\dagger}_{l\sigma}\rangle\rangle^{<}$, $c_{l\sigma} = -\mathrm{i} \int \frac{\mathrm{d}E}{2\pi} \langle\langle d_{l\sigma} d^{+}_{l-\sigma} d_{l-\sigma}, d^{\dagger}_{l\sigma}\rangle\rangle^{<}$. In the Coulomb blockade regime the lesser functions can be calculated according to the equation of motion method [43]. This allows one to express the lesser functions in terms of one- or two-particle retarded (advanced) Green functions. Then, $G^{<}_{l\sigma}$ takes the form: $G^{<}_{l\sigma} = -[(\Gamma^{\mathrm{L}}_l f_{\mathrm{L}} + \Gamma^{\mathrm{R}}_l f_{\mathrm{R}})/(\Gamma^{\mathrm{L}}_l + \Gamma^{\mathrm{R}}_l)](G^{\mathrm{r}}_{l\sigma} - G^{\mathrm{a}}_{l\sigma})$ and similar expression can be written for the two-particle lesser function, whereas the retarded (advanced) ones are calculated from the appropriate equation of motion. Finally, one obtains a set of algebraic equations for one- and two-particle occupation numbers $n_{l\sigma}$, $c_{l\sigma}$, which are solved numerically.

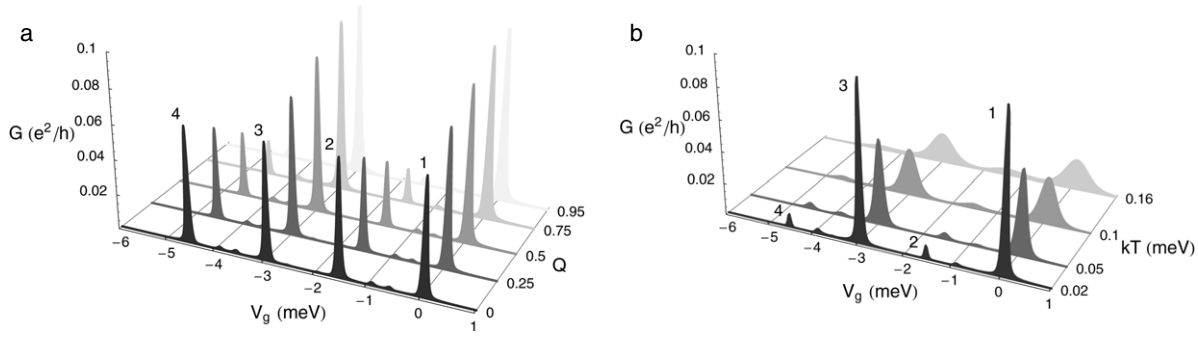

Figure 1. Electrical conductance G as a function of gate voltage for several values of parameter Q (for $kT = 2\Gamma$ (a)) and several values of kT (for $Q = 0.9$ (b)) calculated using the following parameters: $\Gamma = 0.01$ meV, $U_1 = U_2 = 2$ meV, $U_{12} = 1$ meV, $\varepsilon_{10} = -0.05$ meV, $\Delta\varepsilon = \varepsilon_2 - \varepsilon_1 = 0.6$ meV.

3. Numerical results

Numerical calculations of electron and energy transport were performed with use of the following parameters: $\Gamma = 0.01$ meV, $U_1 = U_2 = 2$ meV, $U_{12} = 1$ meV, $\varepsilon_{10} = -0.05$ meV, $\Delta\varepsilon = \varepsilon_2 - \varepsilon_1 = 0.6$ meV and for different values of Q, which characterizes the coupling strength of a given level with external electrodes. Note, that for molecules the coupling strengths of different molecular orbitals to external electrodes may vary strongly due to different spatial distributions of the corresponding wavefunctions [44, 45]. The approach can be also applied to two QDs, with different energy levels ε_1 and ε_2, that are capacitively coupled to each other and attached to external electrodes. The coupling strength to the leads can, then, be varied for each dot separately.

3.1. Electron transport

Although the electric conductance in similar systems has been a subject of many papers, we briefly discuss the problem and present the results obtained for linear conductance $G = e^2 L_0$, so they could be compared with the behaviour of thermal conductance and thermopower. The conductance as a function of gate voltage V_g, which allows one to tune dot energy levels, is presented in figure 1 for several values of Q and several values of kT. For $Q = 0$ the levels are equally coupled with the leads and both levels are active in the electron transport. At low temperatures ($kT = 2\Gamma$) the Coulomb blockade effect is important and thin peaks can be observed when the appropriate energy level crosses the Fermi level in the leads ($\mu = 0$). The intensity of the peak strongly depends on the probability of a given configuration. For $Q = 0$ the conductance shows four high peaks of equal intensity. Peaks 1 and 3 correspond to the situation when either ε_1 or $\varepsilon_1 + U + U_{12}$ crosses the Fermi level in the electrodes. In the first case with ε_1 crossing the Fermi level, the high probability is obtained when both levels are empty, whereas in the second one, with $\varepsilon_1 + U + U_{12}$ crossing the Fermi level, it is obtained when both levels are singly occupied. Similarly, a high intensity can be observed when $\varepsilon_2 + U_{12}$ or $\varepsilon_{12} + U + 2U_{12}$ cross the Fermi level (peaks 2 and 4 in figure 1(a)), as the appropriate configurations with level 1 being singly or doubly occupied are highly probable. On the other hand, the probability of the configuration in which level 1(2) is singly occupied and level 2(1) is empty, is very small for the assumed parameters, so the line corresponding to $\varepsilon_1 + U(\varepsilon_2 + U)$ crossing the Fermi level does not appear in the linear conductance at low temperatures. When Q increases, level 1 becomes strongly coupled to the electrodes and $\Gamma_1 = \Gamma(1 + Q)$, while level 2 is gradually decoupled as $\Gamma_2 = \Gamma(1 - Q)$. Therefore, the intensities of peaks 1 and 3 increase, while 2 and 4 decrease with Q. For $Q = 0.95$ level 2 is practically decoupled and becomes inactive in the transport. Then, electrons are mainly transmitted through empty and singly occupied level 1 which leads to very high and narrow peaks in the conductance (denoted as 1 and 3). With an increase of temperature the peaks become wider and lower (figure 1(b)). Coulomb blockade effects are less significant and are practically negligible for $kT > 16\Gamma$. Instead of single, well separated peaks, a band with broad maxima starts to develop.

3.2. Thermal conductance

The thermal conductance κ, determined from the heat flux $I_Q = -\kappa\Delta T$ under the condition that charge current vanishes, is equal to $\kappa = \frac{1}{T}(L_2 - \frac{L_1^2}{L_0})$ [42]. The conductance calculated as a function of gate voltage for several values of parameter Q is presented in figure 2. At low temperatures ($kT = 2\Gamma$) and $Q = 0$ well-defined peaks can be seen, which are correlated with the peaks in the electrical conductance spectrum (figure 1(a)). However, now the maxima are much wider than those appearing in G. With an increase of Q the peak intensity changes and for high values of Q the spectrum is dominated by peaks 1 and 3, which indicates that states ε_1 and $\varepsilon_1 + U + U_{12}$ are mainly involved in energy transfer due to the strong coupling of level 1 with the electrodes. The influence of temperature on the thermal conductance is presented in figure 3. κ as a function of gate voltage and temperature is depicted in figure 3(a) and several cross-sections corresponding to different values of temperature are given in figure 3(b). At higher temperatures the thermal conductance increases and more states become involved in the transport. The intensities of the peaks as well as their widths increase considerably and finally, for $kT > 16\Gamma$, a wide band develops. Within the band, several peaks corresponding to high values of κ can be observed. The

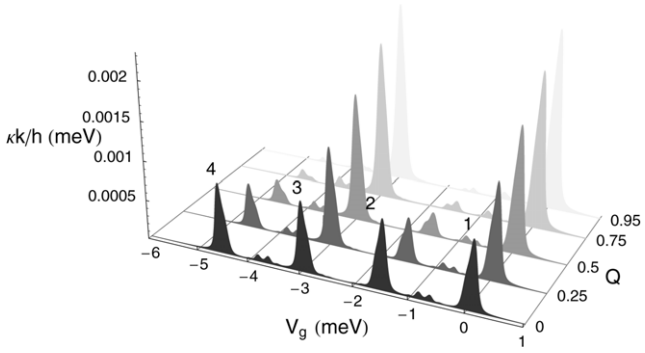

Figure 2. Thermal conductance as a function of gate voltage for several values of parameter Q and $kT = 2\Gamma$. Other parameters as in figure 1.

presented behaviour of κ is considerably different from the dependence found for the charge conductance G depicted in figure 1. The origin of this behaviour can be accounted for as follows. When the temperature is increasing, the thermal distribution of electrons becomes broader and due to different energy weighting tunnelling electrons contribute differently to the charge and heat conductance. Thermal conductance κ increases considerably with temperature as contributions from electrons and holes to the heat conductance add constructively, whereas such contributions to charge conductance compensate. Moreover, additional channels open and contribute to κ, leading to high peaks, which can be easily seen at high temperatures within the wide band. For small gate voltages such a peak appears when the state with energy $\varepsilon_1 + U_{12}$ is close to the Fermi energy. It corresponds to the situation when level 2 is singly occupied. Similarly, at higher gate voltages the heat transport takes place through the channel with energy $\varepsilon_1 + U$ as well as through channel $\varepsilon_1 + U + 2U_{12}$ in which levels ε_1 and ε_2 are singly and doubly occupied, respectively. Although level 2 is weakly coupled to the electrodes a considerable contribution to the high temperature spectrum appears when the state $\varepsilon_2 + U_{12}$ is close to the Fermi energy. The probability of all these states can be enhanced due to temperature. Peaks due to the channels, accessible at high temperatures, are strongly broadened and overlap with each other as well as with a wide and flat band, which evolved from peaks 1 and 3, leading to considerable enhancement of energy transfer. So, they start to dominate the conductance spectrum. On the other hand, due to strong broadening the thermal conductance is relatively low in the region of gate voltages corresponding to peaks 1 and 3. This lowering can be very clearly seen in the middle of the band, as it leads to a valley which practically divides the whole band into two subbands. It should also be noted that for such values of gate voltage the corresponding states are empty or singly occupied, so such configurations are less probable at high temperatures. On the other hand, they give the main contribution to the heat transport at low temperatures. Therefore, due to different probabilities dependent on one- and two-particle occupation numbers certain channels are accessible and take part in the heat transfer, whereas some channels are practically inactive. This selection of accessible channels strongly depends on temperature.

3.3. Thermopower and thermal efficiency

Thermopower S is determined as the voltage drop induced by the temperature gradient, under the condition that the charge current vanishes, $I = 0$. This leads to the following formula for $S = \frac{\Delta V}{\Delta T} = -\frac{1}{eT}\frac{L_1}{L_0}$.

In nanostructures, due to quantum confinement and Coulomb blockade effects the Seebeck coefficient S shows oscillations when the gate voltage is varied [29]. Similar behaviour is obtained for the system under consideration, as presented in figure 4. At low temperatures thermopower varies sharply and ten maxima and minima can easily be seen. The behaviour of S can be explained as follows. When one of the states, say ε_1, approaches the resonance, electrons start to tunnel due to the temperature gradient, which gives rise to a voltage drop under the condition of vanishing current. This voltage drop for the first accessible state with energy ε_1 is positive, but S in units k/e is negative because of the negative electron charge. When ε_1 reaches the resonance, currents due to electrons and holes compensate, so the charge current as well as thermopower vanish at resonance. The situation is similar for other resonant states. Thermopower S changes the

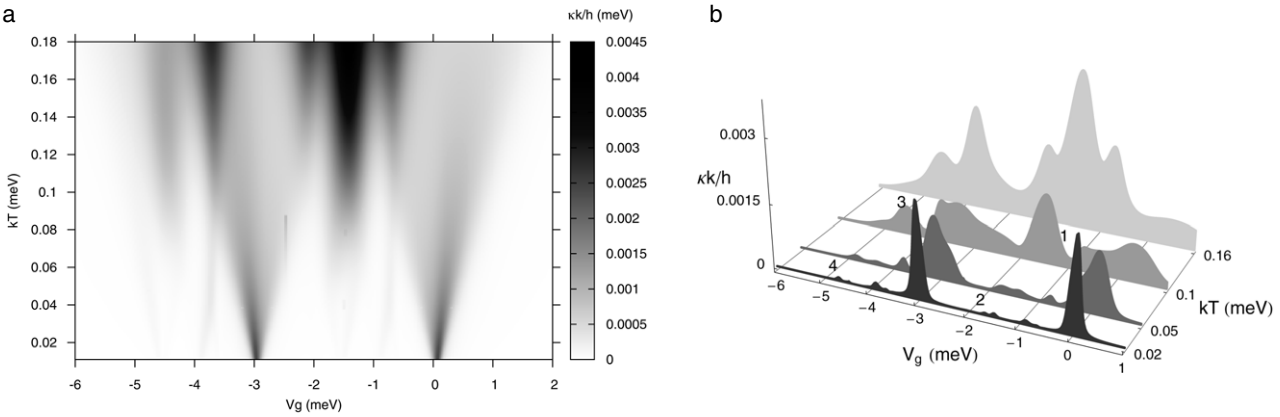

Figure 3. Thermal conductance as a function of gate voltage and temperature for $Q = 0.9$ (a) and cross-sections of κ for several values of kT (b). Other parameters as in figure 1.

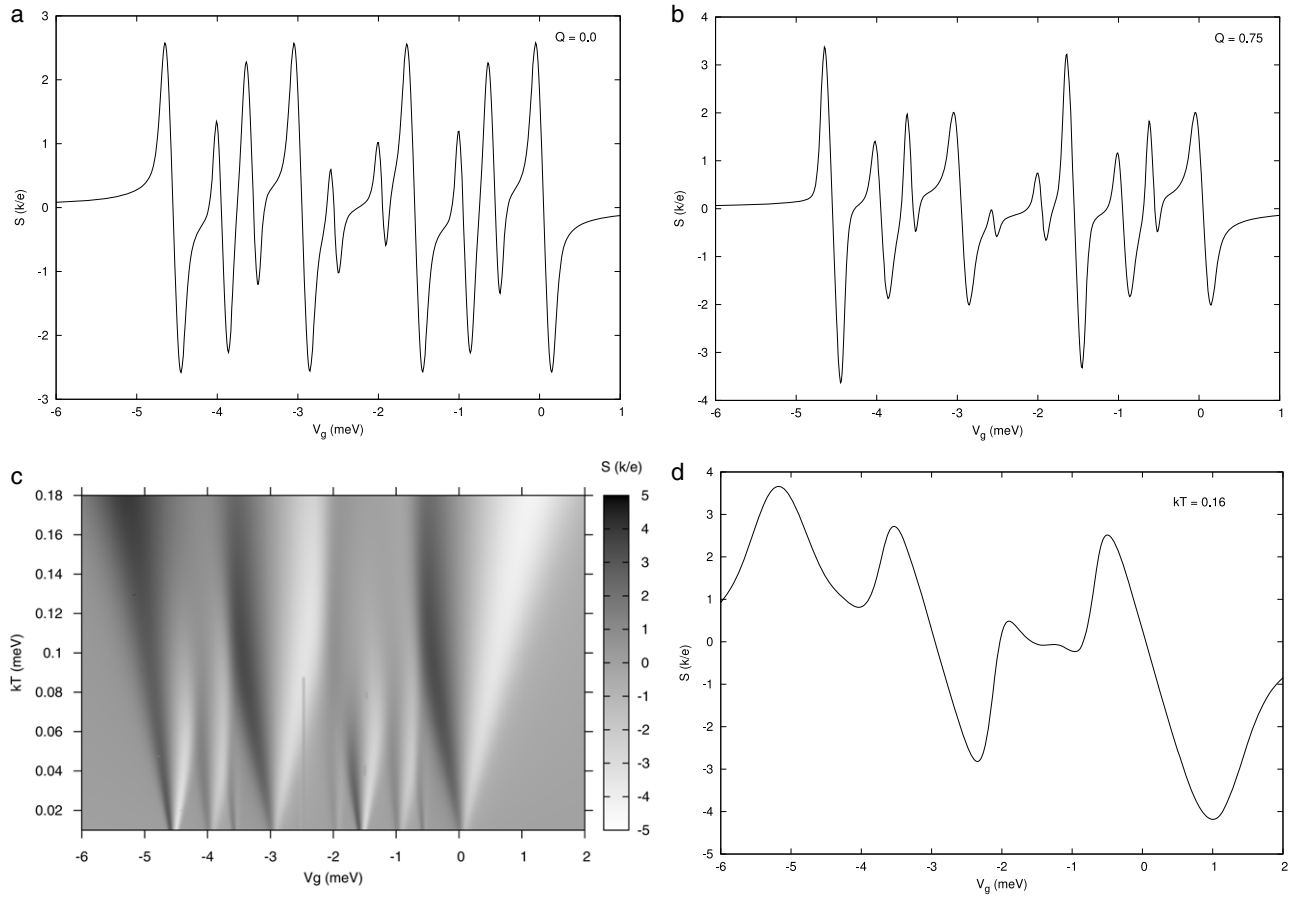

Figure 4. Thermopower as a function of gate voltage for $kT = 2\Gamma$, $Q = 0$ (a) and $Q = 0.75$ (b). Temperature and gate voltage dependence of S for $Q = 0.9$ (c) and cross-section for $kT = 16\Gamma$ (d). Other parameters as in figure 1.

sign, when one of the available states crosses the Fermi energy and for two-level QD twelve such states are possible, which correspond to the poles of the Green function (equation (2)). For the assumed set of parameters only ten different states can appear. Peaks corresponding to all these states are clearly visible in the thermopower spectrum at low temperatures, but their intensities are different and described by the probabilities of particular configurations. For $Q = 0$, similarly as in the electrical conductance G, four peaks dominate (figure 4(a)). However, also those states, which are hardly involved in the conductance contribute to S and lead to well distinguished peaks. In particular, the transmission through the singly occupied level 1 or 2, in the situation when the other one is empty, is low and such configurations hardly contribute to electron or heat transport at low temperatures. However, the appropriate peaks are clearly visible in the thermopower spectrum (two central peaks), although their intensities are considerably lower. When Q increases, level ε_1 becomes strongly coupled to the electrodes leading to the enhancement of the electric conductance (peaks 1 and 3 in figure 1(a)). As a result the appropriate peaks in S are lowered. At the same time level ε_2 is gradually decoupled and transmission through this level is suppressed, leading to a considerable increase of the appropriate peaks in the thermopower spectrum. For higher Q the spectrum is dominated by two peaks corresponding to the states ε_2+U_{12}, ε_2+U+2U_{12} (figure 4(b)). At low temperatures all the peaks are very narrow, but their width increases with temperature, as presented in figures 4(c) and (d). The thermopower then varies gradually, showing broad maxima and minima. At high temperatures a considerable broadening of the distribution function appears. Then the currents due to tunnelling electrons and holes may not compensate exactly at each resonant state. As a consequence the thermopower does not change sign at each resonance. The curve $S(V_g)$ is strongly asymmetric at high temperatures, as depicted in figure 4(d).

The thermal efficiency of the system is expressed in terms of the electrical conductance G, thermal conductance κ and thermopower S as $ZT = \frac{GS^2T}{\kappa}$, which is known as the figure of merit. It is presented in figure 5 for several values of the parameter Q. At low temperatures ($kT = 2\Gamma$) typical double peaks with narrow valleys, corresponding to gate voltages for which thermopower vanishes, can be observed, similarly to systems with single-level dots [39]. However, the number of lines is considerably greater and their intensities are different. For $Q = 0$, both levels are equally coupled to the electrodes, and the four structures which dominate the spectrum are of the same intensity. They correlate well with appropriate peaks in the thermopower and electrical conductance. When Q increases the intensities of all peaks change. The highest intensity is obtained in the situation when the level $\varepsilon_2 + U_{12}$

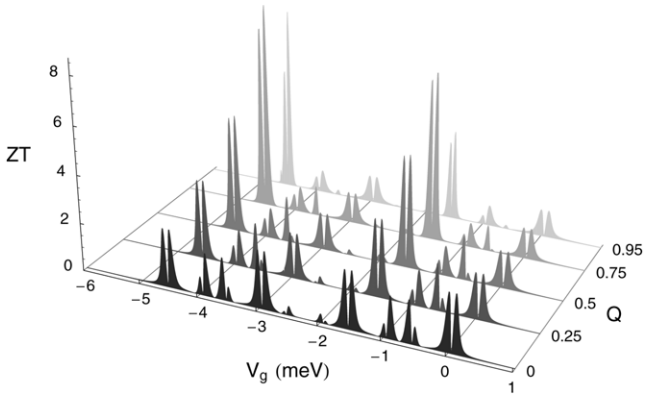

Figure 5. Figure of merit as a function of gate voltage for $kT = 2\Gamma$ and several values of Q. Other parameters as in figure 1.

or $\varepsilon_2 + U + 2U_{12}$ is aligned with the Fermi energy in the leads (figure 5). So, the main contribution to the ZT spectrum comes from level 2, weakly coupled to the external electrodes. ZT is then enhanced due to a considerable increase of the Seebeck coefficient S and moreover, due to suppression of the thermal conductance. The system shows the highest efficiency for $0.75 < Q < 0.95$. Then, the optimal conditions for high efficiency can be fulfilled with small thermal conductance, but relatively high electrical conductance. For larger Q level 2 becomes decoupled from the leads, so the electrical conductance through this level is strongly suppressed and the efficiency of the system with respect to thermoelectricity starts to drop. With an increase of temperature the appropriate structures broaden (figure 6). The intensities of the two peaks, which dominate at low temperatures, become reduced due to a considerable increase of the thermal conductance. At higher temperatures they are relatively small, especially the peak corresponding to the state $\varepsilon_2 + U_{12}$, as the thermal conductance κ in this region of gate voltages is especially high. On the other hand, ZT considerably increases with increasing temperature for small gate voltages. Then, the state ε_1 is active in electrical transport, but the energy transport is strongly suppressed, as presented in figure 3(b). For $kT \approx 16\Gamma$ the ZT spectrum is dominated by the broad peak which develops in this region. The double peak with lines of relatively high intensity, appearing in the spectrum at higher values of V_g, corresponds to the valley in the thermal conductance (figure 3(b)). Therefore, in the system under consideration, the changes of κ with temperature fully determine the ZT spectrum, especially at higher temperatures.

4. Thermoelectric properties of two coupled quantum dots

Up to now, we have discussed thermoelectric coefficients for a QD with two levels ε_1 and ε_2, whose positions were tuned with the gate voltage. The distance between levels $\Delta\varepsilon = \varepsilon_2 - \varepsilon_1$ was treated as a constant. Now, we consider two QDs coupled capacitively, whose levels ε_1 and ε_2, initially aligned and equal to ε_0, are then tuned with additional gate voltages in such a way that they move apart as $\varepsilon_1 = \varepsilon_0 - \tau$ and $\varepsilon_2 = \varepsilon_0 + \tau$. One can also consider two dots coupled via tunnelling processes. The two-dot system then represents an artificial molecule and can be described in terms of the effective two-level dot weakly coupled to external electrodes [46, 47]. New levels, corresponding to the molecule, are usually called the bonding and antibonding ones. In the situation when the levels of both dots were aligned and equal to ε_0, the molecular levels appear at energies $\varepsilon_0 \pm \tau$, with τ describing the coupling strength between the dots. As τ can be easily tuned in an experimental set-up it is reasonable to discuss changes in the thermoelectric spectra when the coupling strength τ is varied. With an increase of τ, the molecular levels move apart. Changes of thermoelectric coefficients with τ and gate voltage, which coherently shift the levels in both dots, are presented in figure 7 for $kT = 2\Gamma$. Assume first that τ is negligibly small. Then, molecular levels are close to each other and four states contribute to transport with one of energies ε_0, $\varepsilon_0 + U_{12}$, $\varepsilon_0 + U + U_{12}$, $\varepsilon_0 + U + 2U_{12}$ crossing the Fermi level in the leads. When the gate voltage is changed successive states become active in the transport, leading to peaks in the electrical conductance (figure 7(a)) and in the thermal conductance (not shown here). The intensities of the peaks are similar. With an increase of τ, tunnelling processes between the dots become important, so the level ε_0 is split and the levels move apart,

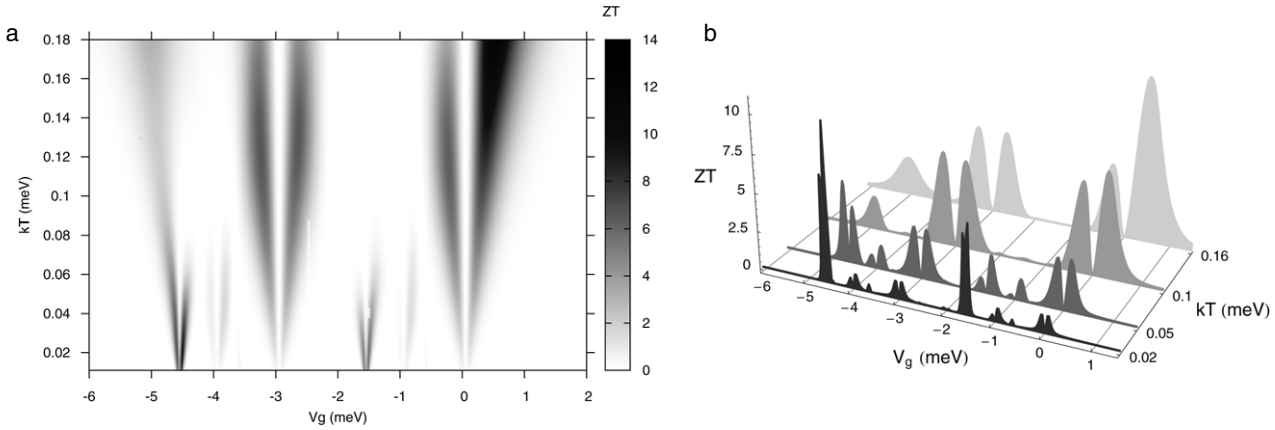

Figure 6. ZT as a function of gate voltages and temperature (a) and cross-sections for several values of kT (b) calculated for $Q = 0.9$. Other parameters as in figure 1.

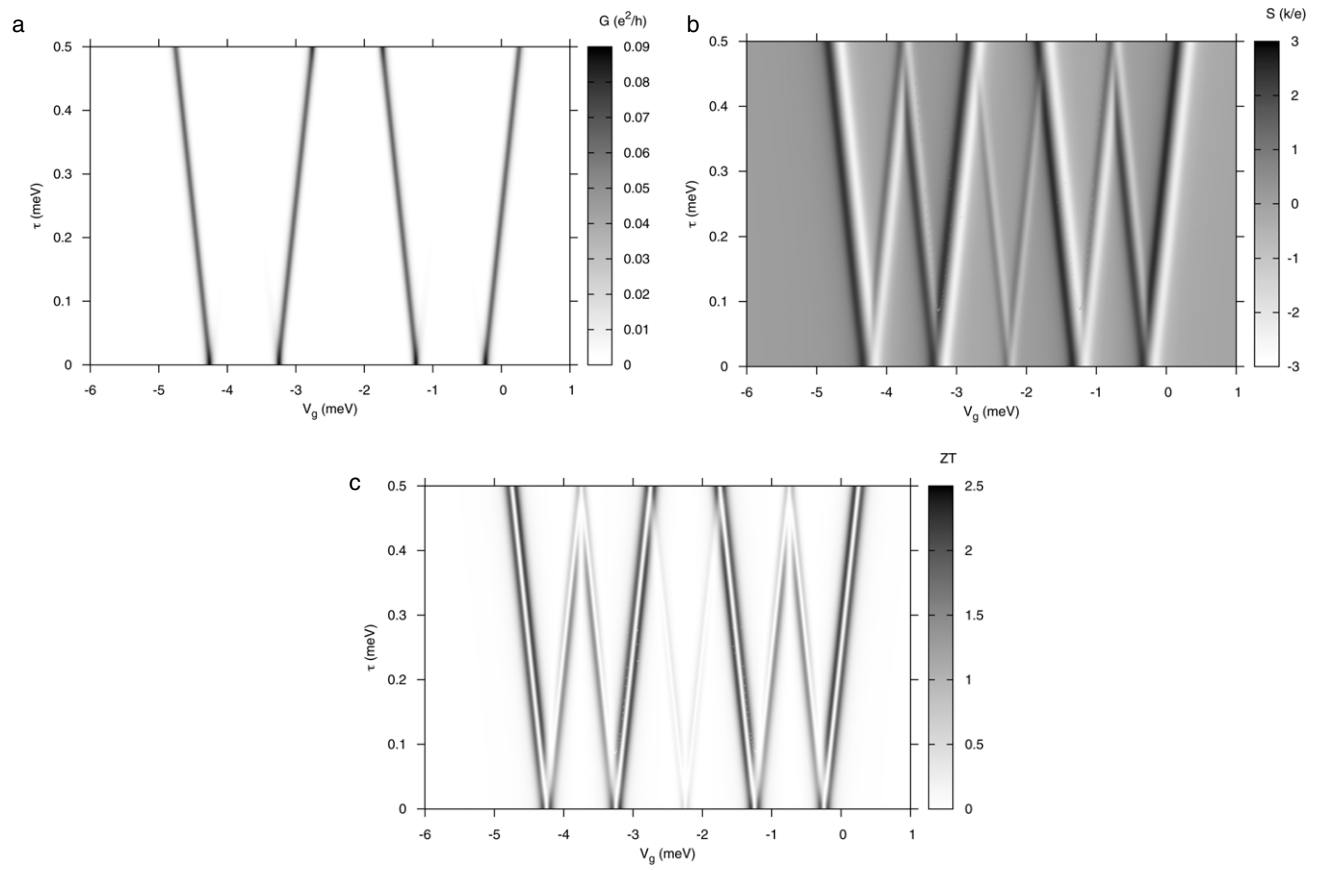

Figure 7. Electrical conductance G (a), thermopower S (b) and ZT (c) in dependence on gate voltage and τ for two QDs. Parameters used: $kT = 2\Gamma$, $Q = 0$, $\varepsilon_0 = 0.25$ meV. Other parameters as in figure 1.

the bonding one to the right and the antibonding one to the left. At low gate voltages (V_g close to zero) the level $\varepsilon_0 - \tau$ is active in the transport, but the antibonding state with energy $\varepsilon_0+\tau$ hardly contributes to the transmission and due to its small intensity the corresponding line cannot be seen in the electrical conductance depicted in figure 7(a). The situation is reversed at higher values of gate voltage.

The low lying bonding state is singly occupied and the probability of transmission through this state is small at low temperatures. Then, unoccupied antibonding state is mainly active in the transport, leading to a high intensity line at energy $\varepsilon_0 + \tau + U_{12}$. With τ increasing this line moves to the left towards higher values of V_g. A similar behaviour can be observed for the Coulomb counterparts of the bonding and antibonding levels. The third peak which can be seen in the conductance G corresponds to the situation when both levels $\varepsilon_0 - \tau$, $\varepsilon_0 + \tau$ are singly occupied and the second electron with opposite spin tunnels through the lower state when the energy $\varepsilon_0 - \tau + U + U_{12}$ approaches the Fermi level. The appropriate line has high intensity and moves to the right with τ increasing. Finally, the last, fourth line corresponds to $\varepsilon_0 + \tau + U + 2U_{12}$ with the bonding state doubly occupied. Although the tunnelling coupling τ between the dots leads to the level splitting, only one of these split states can be active in the transport, leading to the high intensity line in the electrical conductance. The thermal conductance shows a similar behaviour, with line positions correlating well with those in G (not presented here).

Thermopower as a function of gate voltage is depicted in figure 7(b). It oscillates with V_g and shows several maxima and minima of different intensities. The splitting of the levels with increasing τ can be clearly seen. The intensities of the peaks are different. The highest intensity corresponds to these four peaks which dominate the linear conductance. However, antibonding (bonding) states, empty or singly occupied, which are almost inactive in electron transport, contribute considerably to the thermopower, leading to well-defined peaks. Moreover, in the centre of the spectrum two additional peaks develop. They correspond to the situation when an electron tunnels through the occupied bonding or antibonding state, whereas the second state is empty. Probabilities of such configurations are low, so the intensities of the lines are also low.

Similar behaviour is seen for the figure of merit ZT in which ten double lines can be seen for intermediate values of τ (figure 7(c)). There are four such lines with high intensity, two corresponding to bonding states and two for antibonding ones, as well as four lines with lower intensity. Finally in the centre of the spectrum two additional lines with small intensity correspond to transport through occupied states. The peak intensity hardly changes along a given line when the coupling between dots is changed. The presented results show that in two-dot systems the probability of a given configuration with an electron occupying the bonding or antibonding state plays an important role and strongly influences the line intensities

in the spectrum. The line position can be easily manipulated when τ is varied.

5. Summary and discussion

Here, we have studied the electrical and thermal properties of quantum dots attached to external electrodes. The approach, based on the Green function formalism, allows us to determine the probabilities of various configurations accessible for the system with two levels active in the transport. These temperature-dependent weights strongly influence the transport properties. Additional selection of channels active in the transport can be obtained for a molecule due to a level-dependent coupling strength with external electrodes, described here by the parameter Q. Such a selection can lead to a negative differential conductance G_{diff}, as well as essentially influencing the energy transfer. At low temperatures, owing to Coulomb blockade effects, well-defined peaks develop in the thermal conductance with their intensity strongly depending on the parameter Q. At high temperatures, peaks in κ evolve in the wide band, but with large maxima and deep valleys, so that channels with strongly reduced energy transfer can be found. In these regions of gate voltage the tendency towards thermoelectricity is considerably enhanced and optimal conditions for the effect are fulfilled, as the thermal conductance is relatively low, while the thermopower and electrical conductance are quite high. There is the possibility of strong modifications of ZT when parameter Q is changed. The study presented shows that the physics of multilevel dots is much richer than for the case of single-level dots and moreover, a considerable enhancement of thermoelectric efficiency can be obtained.

References

[1] Christensen M, Abrahamsen A B, Christensen N B, Juranyi F, Andersen N H, Lefmann K, Anderasson J, Bahl C R H and Iversen B B 2008 *Nat. Mater.* **7** 811

[2] Joshi G, Lee H, Lan Y, Wang X, Zhu G, Wang D, Gould R W, Cuff D C, Tang M Y, Dresselhaus M S, Chen G and Ren Z 2008 *Nano Lett.* **8** 4670

[3] Kim W, Singer S L, Majumdar A, Vashaee D, Bian Z, Shakouri A, Zeng G, Bowers J E, Zide J M O and Gossard A C 2006 *Appl. Phys. Lett.* **88** 242107

[4] Venkatasubramanian R, Siivola E, Colpitts T and O'Quinn B 2001 *Nature* **413** 597

[5] Hicks L D, Harman T C, Sun X and Dresselhaus M S 1996 *Phys. Rev.* B **53** R10493

[6] Reddy P, Jang S Y, Segalman R A and Majumdar A 2007 *Science* **315** 1568

[7] Hochbaum A I, Chen R, Delgado R D, Liang W, Garnett E C, Najarian M, Majumdar A and Yang P 2008 *Nature* **451** 163

[8] Baheti K, Malen J A, Doak P, Reddy P, Jang S Y, Tilley T D, Majumdar A and Segalman R A 2008 *Nano Lett.* **8** 715

[9] Boukai A I, Bunimovich Y, Tahir-Kheli J, Yu J K, Goddard W A III and Heath J R 2008 *Nature* **451** 168

[10] Schwab K, Henriksen E A, Worlock J M and Roukes M L 2000 *Nature* **404** 974

[11] Uchida K, Takahashi S, Harii K, Ieda J, Koshibae W, Ando K, Maekawa S and Saitoh E 2008 *Nature* **455** 778

[12] Murphy P, Mukerjee S and Moore J 2008 *Phys. Rev.* B **78** 161406(R)

[13] Finch C M, Garcia-Suarez V M and Lambert C J 2009 *Phys. Rev.* B **79** 033405

[14] Gravier L, Serrano-Guisan S, Reuse F and Ansermet J P 2006 *Phys. Rev.* B **73** 024419
Gravier L, Serrano-Guisan S, Reuse F and Ansermet J P 2006 *Phys. Rev.* B **73** 052410

[15] Ludoph B and Ruitenbeek J M 1999 *Phys. Rev.* B **59** 12290

[16] Godijn S F, Moller S, Buchmann M, Molenkamp L W and van Langen S A 1999 *Phys. Rev. Lett.* **82** 2927

[17] Yonatan D and Di Ventra M 2009 *Nano Lett.* **9** 97

[18] Markussen T, Jauho A P and Brandbyge M 2009 *Phys. Rev.* B **79** 035415

[19] Galperin M, Nitzan A and Ratner M A 2008 *Mol. Phys.* **106** 397

[20] Lunde A M, Flensberg K and Glazman L I 2006 *Phys. Rev. Lett.* **97** 256802

[21] Segal D 2005 *Phys. Rev.* B **72** 165426

[22] Pauly F, Viljas J K and Cuevas J C 2008 *Phys. Rev.* B **78** 035315

[23] Wang B, Xing Y, Wan L, Wie Y and Wang J 2005 *Phys. Rev.* B **71** 233406

[24] Beenakker C W J and Staring A A M 1992 *Phys. Rev.* B **46** 9667

[25] Blanter Y M, Bruder C, Fazio R and Schoeller H 1997 *Phys. Rev.* B **55** 4069

[26] Turek M and Matveev K A 2002 *Phys. Rev.* B **65** 115332

[27] Koch J, von Oppen F, Oreg Y and Sela E 2004 *Phys. Rev.* B **70** 195107

[28] Kubala B and Konig J 2006 *Phys. Rev.* B **73** 195316

[29] Kubala B, Konig J and Pekola J 2008 *Phys. Rev. Lett.* **100** 066801

[30] Zianni X 2007 *Phys. Rev.* B **75** 045344

[31] Boese D and Fazio R 2001 *Europhys. Lett.* **56** 576

[32] Dong B and Lei X L 2002 *J. Phys.: Condens. Matter* **14** 11747

[33] Krawiec M and Wysokinski K I 2006 *Phys. Rev.* B **73** 075307

[34] Sakano R, Kita T and Kawakami N 2007 *J. Phys. Soc. Japan* **76** 074709

[35] Scheibner R, Buchmann H, Reuter D, Kiselev M N and Molenkamp L W 2005 *Phys. Rev. Lett* **95** 176602

[36] Yoshida M and Oliveira L N 2009 arXiv:0904.2326 [cond-mat.mes-hall]

[37] Tsaousidou M and Triberis G P 2007 *ICPS 2006: 28th Int. Conf. on the Physics of Semiconductors*; *AIP Conf. Proc.* **893** 801

[38] Dubi Y and Di Ventra M 2009 *Phys. Rev.* B **79** 081302

[39] Swirkowicz R, Wierzbicki M and Barnaś J 2009 *Phys. Rev.* B **80** 195409

[40] Chang Y C and Kuo D M T 2008 *Phys. Rev.* B **77** 245412

[41] Kuo D M T and Chang Y C 2007 *Phys. Rev. Lett.* **99** 086803

[42] Mahan C D 2000 *Many-Particle Physics* (New York: Plenum)

[43] Niu C, Lin D L and Lin T H 1999 *J. Phys.: Condens. Matter* **11** 1511

[44] Hettler M H, Schoeller H and Wenzel W 2002 *Europhys. Lett.* **57** 571

[45] Thielmann A, Hettler M H, Konig J and Shon G 2005 *Phys. Rev.* B **71** 045341

[46] Kostyrko T and Bulka B 2005 *Phys. Rev.* **71** 235306

[47] Fransson J and Eriksson O 2004 *Phys. Rev.* B **70** 085301